Clays and Clay Minerals, Vol. 46, No. 2, 204–214, 1998.

GEOCHEMISTRY AND PARAGENESIS OF HEULANDITE CEMENTS IN A MIOCENE MARINE FAN-DELTA SYSTEM OF THE POHANG BASIN, REPUBLIC OF KOREA

JIN HWAN NOH

Department of Geology, Kangwon National University, Chuncheon 200-701, Republic of Korea

Abstract—In the Pohang area of Korea, heulandite occurs as cements in conglomerate and sandstone of a Miocene marine fan-delta system resting on Eocene dacitic volcanics. Three types of heulandite cements are distinguishable in the fan-delta sediments on the basis of texture, chemical composition and authigenic mineral association. The earliest type I heulandite (Si/(Al+Fe): 3.5–3.8) occurs as microcrystalline (10–30 μm) *in situ* crystallites that replace volcanic matrix and are intermixed with early-formed smectite. Type II heulandite (Si/(Al+Fe): 3.2–3.6) occurs as medium-grained (30–60 μm) crystal aggregates rimming intergranular cavities. Type III heulandite (Si/(Al+Fe): 3.6–4.1) is the last to form and is a composite phase of heulandite–clinoptiloite, which occurs as unusually coarse (50–200 μm) single-crystal cement associating with late-formed smectite and hematite.

These characteristic heulandite cements were formed by alteration of volcaniclastic sediment during shallow burial (burial temperature: 40–60 °C) and uplift in marine pore fluid diluted by meteoric water. Sr isotope data for heulandite II ($^{87}Sr/^{86}Sr$: 0.706565–0.706598) and heulandite III ($^{87}Sr/^{86}Sr$: 0.707347–0.707432) indicate that the pore fluid was progressively mixed with meteoric water during burial and uplift but the Ca in the pore-filling heulandites has been derived mainly from dissolution of carbonate cements. Heulandite III, heulandite–clinoptilolite, was formed with an unusual coarsening and chemical zoning at somewhat diluted and disequilibrium conditions caused by the migration of oxygen-rich meteoric water during or after uplifting.

Key Words—Burial, Fan-delta, Heulandite Cement, Heulandite–Clinoptilolite, Meteoric Water, Sr Isotope, Uplift, Volcaniclastic.

INTRODUCTION

Zeolite occurrences in sedimentary rocks are remarkably similar in that they are commonly found as *in situ* alterations of the glassy matrix of pyroclastic rocks. The most common type of zeolites that occurs in volcaniclastic rocks is the heulandite-group, that is, heulandite and clinoptilolite, of which the upper range of thermal stability tends to be less than about 100 °C (Iijima and Utada 1971; Surdam and Boles 1979; Noh and Boles 1993). Ground water control of clinoptilolite formation has been recently reported in tuffaceous rocks undergoing very low-temperature (27–55 °C) burial diagenesis (Lander and Hay 1993). In most cases, however, the heulandite-group zeolites from tuffaceous rocks are usually found as very fine-grained (mostly less than 10 μm) aggregates, commonly accompanying smectite (Hay 1966; Surdam and Boles 1979; Noh and Boles 1989; Lander and Hay 1993; Noh and Boles 1993). It is well known that heulandite and clinoptilolite are nearly isostructural but varying in chemical composition (Gottardi and Galli 1985). An association of heulandite and clinoptilolite in the same rock or their single composite phase, such as a zoned crystal, has not been found in any rock system, though a compositionally zoned clinoptilolite was reported in the Barstow tuffs (Sheppard and Gude 1969).

Coarse-grained sediments are of some interest because they have initially high porosity–permeability which can allow considerable mass transfer. However, very little is known about the diagenetic mineral facies as well as zeolite occurrence in coarse-grained sediments of alluvial fan and fan-delta systems. Various authigenic heulandites were recently identified in the middle Miocene conglomeratic formation of a marine fan-delta system in the Pohang area, Korea. An unusual characteristic of the deposit is that heulandite and a composite phase of heulandite and clinoptilolite occur as coarse-crystalline intergranular cements in the non-glassy, but partially volcaniclastic, conglomerate and sandstone. This study illustrates a new mode of occurrence, paragenesis and geochemistry of the heulandite and heulandite-clinoptilolite cements from a fan-delta system, using textural, high-temperature X-ray diffraction (XRD), chemical and Sr isotope analyses.

MATERIALS AND METHODS

Representative samples of conglomerate and sandstone were collected from roadside cuttings through trenching of outcrop surface to a depth of about 20–30 cm. Some unconsolidated samples were obtained by impregnation with quick-curing epoxy in the field.

For the isotopic analyses of heulandite cements, purified samples were obtained by: 1) disaggregating of samples by light crushing and ultrasonic vibrating in distilled water, 2) obtaining a 100–300 mesh size frac-

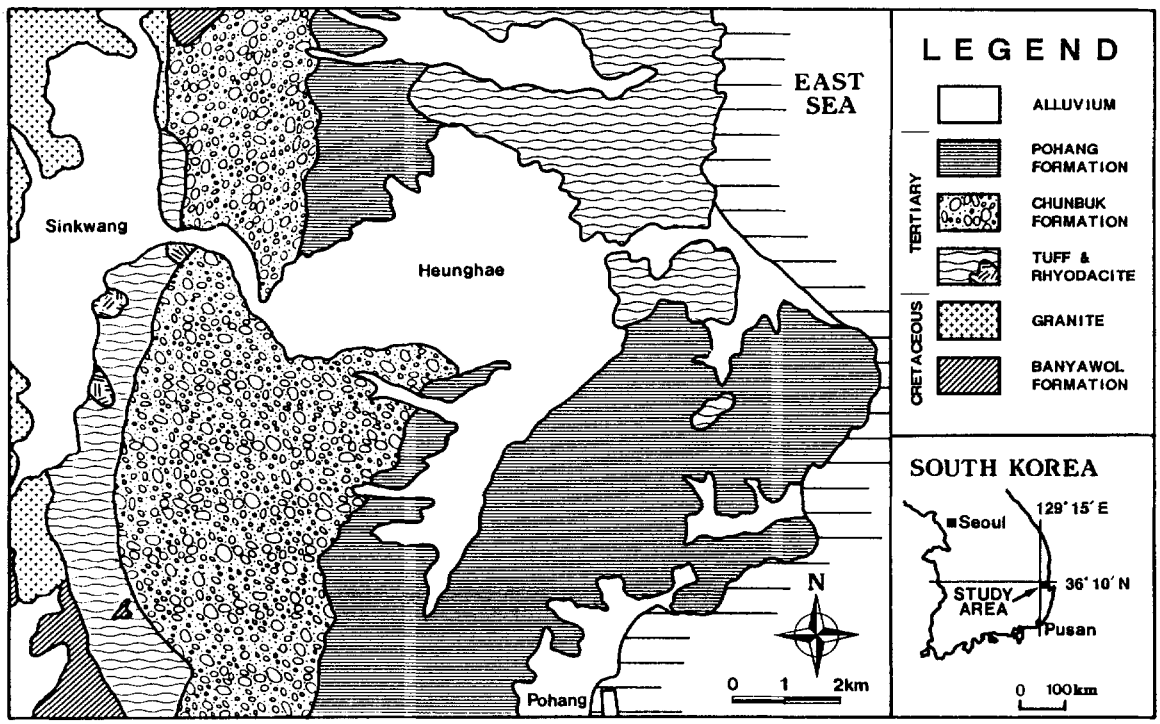

Figure 1. Geologic and index maps of Pohang area.

tion by wet sieving, 3) heavy liquid separation by dibromomethane (CH_2Br_2, S.G.: 2.48) and 4) further purification by hand-picking under the binocular microscope. Separation quality of the samples was optically checked by the preparation of grain sections with immersion oil. All the samples treated with heavy liquid and immersion oil were washed by acetone, 1:1 solution of ethanol and water and liquid soap, followed by drying at the temperature less than 40 °C in an oven.

Petrographic observations are based on more than 200 thin sections of sandstones and sandy matrix of conglomerates. Identification of bulk mineralogy and concentrated authigenic phases such as heulandite and smectite were based on XRD analyses. A phase transition of heulandite at elevated temperatures up to 600 °C was traced by using high-temperature XRD apparatus at the heating rate of 10 °C/min.

Heulandite and other authigenic minerals were analyzed by an electron microprobe with 5 wavelength dispersive spectrometers (WDS) at conditions of 15 kV and 10 nA with a beam size of 5 μm. The $^{87}Sr/^{86}Sr$ ratios were measured at Korea Basic Science Institute on a VG 54-30 thermal ionization mass spectrometer. In addition, strontium concentrations for heulandite, carbonates and volcanic rocks were determined by an atomic absorption spectrophotometric analysis.

GEOLOGIC SETTING AND LITHOLOGY

The Pohang Basin located in the southeastern margin of the Korean Peninsula, that is, the Pohang area, consists of the Miocene Yeonil Group (Figure 1). The Pohang Basin has undergone rapid subsidence (about 700 m/my) during middle Miocene time and was uplifted in the late Miocene (Chough and Barg 1987; Hwang and Chough 1990). The basement of the basin is composed of Cretaceous granite, hornfelsic metasedimentary rocks (Banyawol Formation) and Eocene extrusives (K-Ar age: 41.77–46.24 Ma) of dacitic composition (Noh 1994). The Eocene volcanics (rhyodacite, dacite and subordinating tuffs) underlie and are in contact with Yeonil Group by faulting and unconformity.

The Yeonil Group dips gently eastward and consists of the Chunbuk Formation and overlying Pohang Formation. The thickness of the Miocene sedimentary rocks has been estimated at between 600 and 800 m. The Chunbuk Formation, whose thickness ranges from 300 to 500 m, consists mostly of coarse-grained epiclastic units, including agglomerate, gravelstone, conglomerate and pebbly sandstone. The formation was deposited as a fan-delta (Chough et al. 1990; Hwang and Chough 1990). Stratigraphy and lithofacies of the fan-delta system were recently documented by Hwang (1993). The proximal facies of this system is nonmar-

https://doi.org/10.1346/CCMN.1998.0460211 Published online by Cambridge University Press

Table 1. Different heulandite cements and their characteristic features.

Type	Crystal size	Texture	Si/(Al+Fe)	Comments
Heulandite I	10–30 μm	Microcrystalline random aggregates	3.8–3.8	Rare, *in situ* crystallites of glassy matrix, residuals in calcite cement
Heulandite II	30–60 μm	Cavity-rimmings & interstitial fillings	3.2–3.6	Abundant, undulatory extinction, sometimes with smectite coatings
Heulandite III	50–200 μm	Single-crystal intergranular cement	3.6–4.1	Common, mostly zoning, composite phase of heulandite and clinoptilolite, smectite inclusion common, sometimes with hematite coatings

ine and coarser-grained. At least 3 small-scale fans are locally superimposed to form composite discontinuous stratigraphic units of terrigenous sediments. The overlying Pohang Formation is composed of fine-grain pelagic to hemipelagic marine sediments.

Sediments of the Chunbuk Formation were undoubtedly derived from the Cretaceous basement rocks and the Eocene volcanic masses that are exposed in the western margin of the study area (Noh 1994). Outsized coarse clasts consist mostly of the Cretaceous granite and metasedimentary rocks such as hornfels. Pebble- to cobble-sized detritus of volcanic origin are also found in the fan-delta system, but their presence is locally limited and uncommon.

In comparison to the low volcanic proportion in pebbles and cobbles of conglomerates, sandstones and sandy matrix of conglomerates of the fan-delta formation usually contain higher amount of volcanic detritus. Volcanic rock fragments made up mostly of the Eocene rhyodacite, dacite and basalt are commonly included in sandstones and sandy matrix of conglomerates, together with some phenocryst fragments such as corroded quartz and euhedral feldspar grains indicative of volcanic origin. But the proportion of these volcanic detritus is no more than 10% in point-count analysis. In addition, no type of pyroclastic material, such as glass shards and pumice fragments, is found in these fan-delta sediments.

Sandstones and sandy matrix of conglomerates of the fan-delta system range in composition from lithic arkose to feldspathic litharenite. These are characterized by a subequal proportion of quartz and feldspar and a dominance of alkali feldspars, made up of orthoclase, sanidine and perthite, over plagioclase. Mafic mineral grains are nearly absent, but rare biotite flakes are locally common.

The Pohang Formation, 200–300 m thick, is composed mainly of mudstone and shale. Thin beds of channelized sandstone are embedded locally in the formation, but are very limited in occurrence. Siliceous mudstone whose matrix chiefly consists of opal-CT and authigenic quartz is dominant in the formation. Several units of siliceous shale, which usually contain abundant plant fossils, are intercalated in the formation, and are commonly interbedded with the mudstone in the upper part of the formation. Dolomite concretions ranging from 1–3 m in diameter are common in the mudstone units and occur in more than 10 horizons throughout the formation. Diatomaceous beds are sparsely interbedded in the middle to upper part of the formation.

OCCURRENCE OF HEULANDITE AND OTHER AUTHIGENIC MINERALS

Heulandite occurs as coarsely crystalline (0.01–0.2 mm) cement in conglomerate and sandstone of the Chunbuk Formation. Compared to other heulandite occurrences in tuffs and volcaniclastic sandstones (Hay 1966; Surdam and Boles 1979; Noh and Boles 1993), the heulandite from the fan-delta system is unusually coarsely crystalline. The heulandite cements are commonly found in all the coarse-grained fan-delta facies, but the zeolite is locally absent in reworked channelized sandstone facies and transitional facies of the fan-delta system. Smectite and calcite instead occur there as the main authigenic minerals.

Heulandite is mostly found as coffin-shaped crystals or crystal aggregates within intergranular pore spaces. The heulandite cements can be divided into 3 types on the basis of texture, crystallinity and the mode of occurrence: 1) early-formed microcrystalline (10–30 μm) aggregates (heulandite I), 2) intermediate-formed (30–60 μm) crystals-rimmings (heulandite II) and 3) late coarsely crystalline (50–200 μm) intergranular cements (heulandite III) (Table 1). The 3 types do not show any striking lateral zoning in relation to lithology and sedimentary facies, although vertical zoning could not be checked due to lack of available core samples.

Heulandite I is relatively rare, compared to heulandite II and III. The heulandite I is found as *in situ* replacements and/or precipitates at the expense of interstitial glassy and clayey matrix (Figure 2A). Petrographic observations indicate that dacitic to rhyodacitic groundmass materials appear to be major constituents of the original matrix in the zeolite-containing sandstone and conglomerate. Other pyroclastic substances such as glass shards are not found in the matrix. The complexity in the composition of the original matrix seems to be related to weathering effects and diverse sediment input source prior to deposition. However, despite the fact that the fan-delta sediments are not typical volcaniclastic deposits, the mode of oc-

https://doi.org/10.1346/CCMN.1998.0460211 Published online by Cambridge University Press

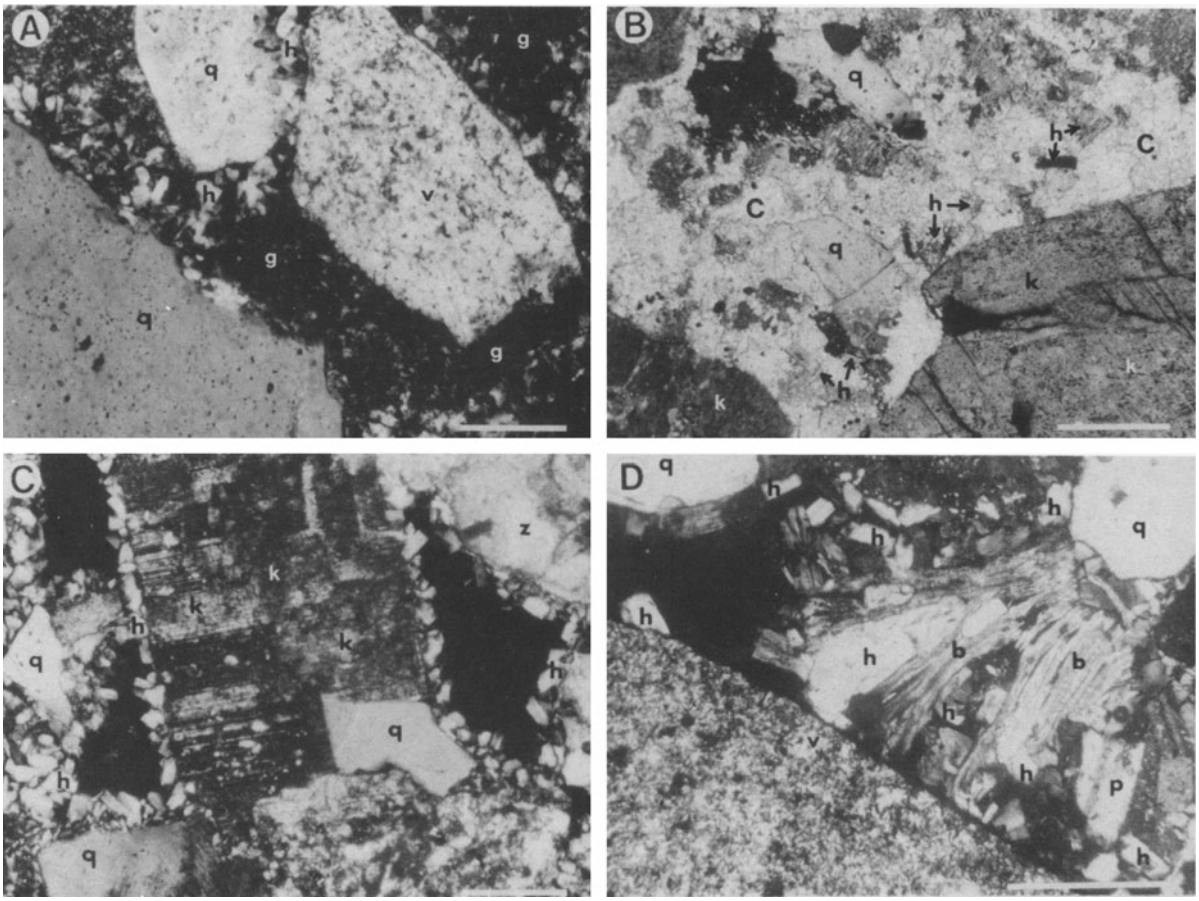

Figure 2. Photomicrographs showing the mode of occurrence of heulandite cements (heulandite I and II) in conglomerates and sandstones in crossed nicols (Scale bars are 0.1 mm). A) Fine-grained heulandite (h) cements (heulandite I) formed at the expense of incipient of glassy matrix (g, dark) between detrital grains of quartz (q) and volcanic rock (r). B) Heulandite (h, heulandite I) remnants replaced by calcite (c) cements: quartz (q) K-feldspar (k). C) Crystallization of medium-grained heulandite (h, heulandite II) rimming framework grains of K-feldspar (k), quartz (q) and clinozoisite (z). D) Cavity-filling of heulandite (h, heulandite II) within deformed biotite flakes (b), and detrital grains of quartz (q) and volcanic rock (v).

currence of heulandite I is similar to those reported in volcaniclastic sandstones from other areas (Surdam and Boles 1979; Noh and Boles 1993). The heulandite I occurs locally as remnants in the calcite-cemented sandstone and conglomerate (Figure 2B), which implies an early formation of the heulandite.

Heulandite II, the most common type in the study area, occurs as rims and fillings of interstitial cavities (Figure 2C). Sometimes it occurs as a coarse-grained open-space filling within deformed mica flakes (Figure 2D). Heulandite II usually does not accompany smectite, but if smectite is present in the heulandite aggregates, it occurs as a late coating on the heulandite (Figure 3A). This indicates that heulandite II formed prior to the late-formed smectite precipitation. Equigranular euhedral crystals that exhibit undulatory extinction are characteristic of heulandite II.

Heulandite III, which is compositionally corresponding to a heulandite–clinoptilolite phase, occurs as very coarse-crystalline cements (Figure 3B). The heulandite III has a broad crystal size distribution (0.05–0.2 mm), compared to the other types of heulandite. It is unusual and characteristic in the mode of heulandite occurrence that the heulandite III sparsely cements detrital grains as a large single-crystal cement (Figures 3B, 3C, 3D). The heulandite III crystallizes and perches onto the smectite coating, commonly along the outline of detrital grains (Figures 3B, 3C), though the smectite coatings tend to pinch out between the heulandite and detrital grains. In addition, smectite is sometimes found as an inclusion within the heulandite cement. This type of heulandite sometimes occurs in association with pigment-like hematite or with a smectite–hematite mixture. The heulandite usually shows an optical zoning with nearly isotropic feature in the inner part of the each crystal (Figures 3C, 3D).

Calcite, dolomite, pyrite, smectite and gypsum are identified as the early-formed authigenic phases in the

https://doi.org/10.1346/CCMN.1998.0460211 Published online by Cambridge University Press

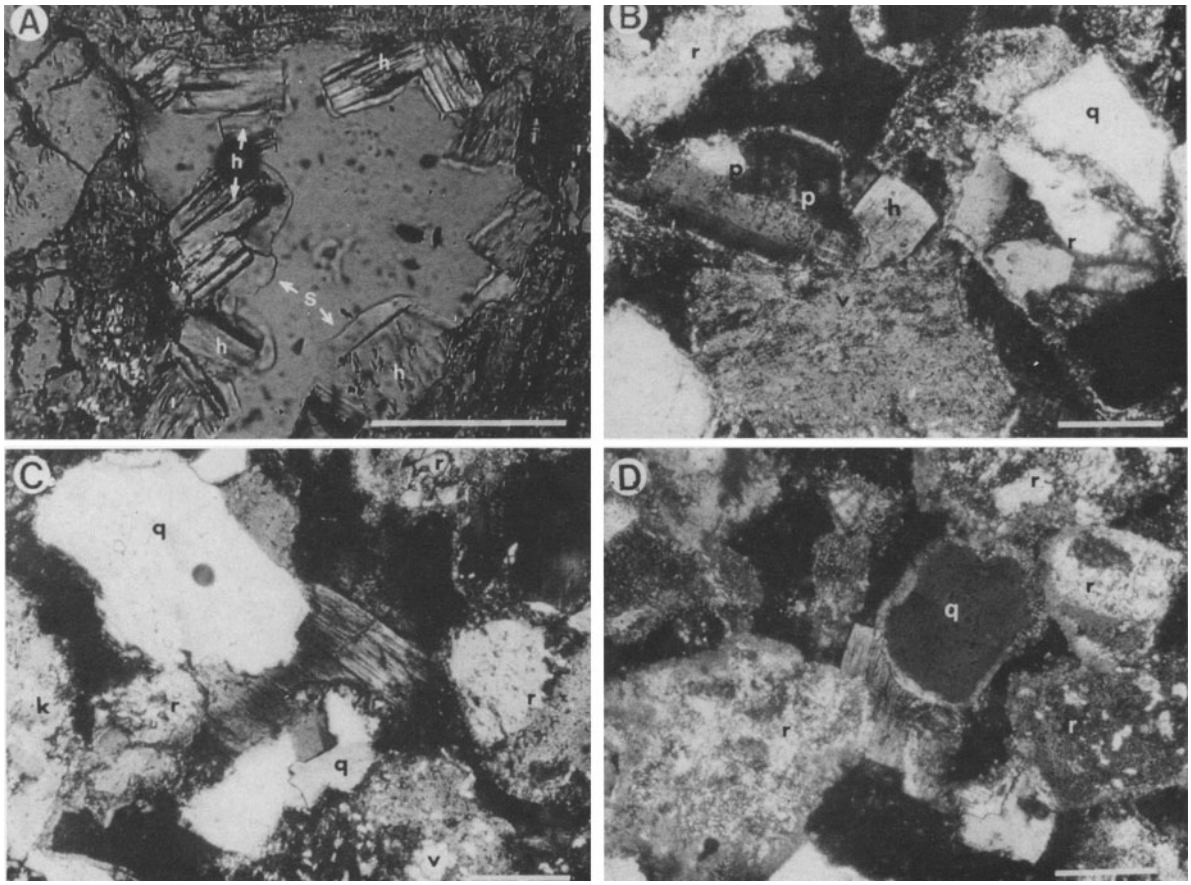

Figure 3. Photomicrographs showing the mode of occurrence of heulandite cements (heulandite II and III) in conglomerates and sandstones in crossed nicols (Scale bars are 0.1 mm). A) Cavity-filling of medium-grained heulandite (h, heulandite II) coated with smectite: Nicols are subparallel. B) Coarse-grained heulandite (h, heulandite III) sparsely filling the interstitial pore space (dark) outlined by smectite coatings (bright): detrital quartz (q), plagoclase (p), volcanic rock (v) and unknown igneous rock fragments (r). C) A large heulandite (heulandite III) cementing detrital grains of quartz (q), K-feldspar, volcanic (v) and unknown rock fragments: Note the lower interference color in the central part, compared to the outside of the heulandite crystal. D) A single-crystal cement of heulandite (heulandite III) filling the detrital grains of quartz (q) and rock fragments (r) coated with the mixture of smectite and hematite. Note the pinching out of smectite coatings within the interfaces of the heulandite and detrital grains.

heulandite-deficient sandstones and conglomerates of the Chunbuk Formation. In addition to the early-formed smectite associating with heulandite I, the late-formed smectite, of which the precipitation stage is intermediate between heulandite II and III, is also found in the zeolite-bearing samples. Gypsum occurs separately from calcite and pyrite. The early carbonate cements of either micritic or crystalline calcite are ubiquitous throughout the formation. In the mudstone and shale of the Chunbuk Formation, smectite and opal-CT constitute the major authigenic phases.

Heulandite was not identified in the Pohang Formation. Instead, the opal-CT + smectite is the dominant authigenic assemblage in the siliceous mudstone and shale. Either gypsum or pyrite occurs as minor authigenic phases. Micritic dolomite accompanying small amounts of pyrite is characteristic of the carbonate concretions within the mudstones. Calcite and opal-CT form late vein-fill in the early-formed dolomite matrix of septarian concretions.

HEULANDITE CHEMISTRY

Heulandite–clinoptilolite is a solid solution series in terms of crystal-chemical aspects, having significant differences in Si/Al ratio and cation content (Alietti 1972; Boles 1972; Gottardi and Galli 1985). However, the zeolite group behaves differently upon heating, depending on chemical composition. This has been used to distinguish heulandite from clinoptilolite (Mumpton 1960; Boles 1972; Alietti et al. 1974).

Chemical composition of major elements of the heulandite was obtained by an electron microprobe analysis. The data were screened in accordance with the suggested balance error criteria (E% $<$ 10%) by Got-

https://doi.org/10.1346/CCMN.1998.0460211 Published online by Cambridge University Press

Table 2. Representative electron microprobe analyses (wt%) of heulandites and their chemical formulae.

	Heulandite I			Heulandite II			Heulandite III			
							Core		Rim	
	I-1	I-2	I-3	II-1	II-2	II-3	III-1	III-2	III-3	III-4
SiO_2	64.47	62.40	60.92	64.40	63.75	63.33	66.25	66.96	61.82	64.11
Al_2O_3	14.32	14.51	15.59	15.69	15.77	15.74	13.86	13.92	13.83	14.27
Fe_2O_3†	0.04	0.00	0.10	0.32	0.04	0.25	0.13	0.00	0.08	0.06
MgO	1.62	1.48	1.20	1.80	1.58	1.64	1.66	1.33	1.30	1.38
SrO	0.11	0.31	0.00	0.50	0.24	0.79	0.17	0.17	0.00	0.00
CaO	4.84	4.96	6.16	4.72	4.87	4.57	4.33	4.89	4.17	4.48
Na_2O	0.13	0.11	0.16	0.29	0.19	0.24	0.18	0.30	0.34	0.61
K_2O	0.68	0.92	0.79	1.02	0.11	1.32	0.68	0.70	1.21	1.20
Total	86.21	84.69	84.92	89.01	87.55	87.88	87.25	88.41	82.75	86.15
					72 oxygens					
Si	28.56	28.28	27.60	27.88	27.98	27.83	28.92	28.92	28.59	28.53
Al	7.48	7.75	8.33	8.14	8.16	8.15	7.13	7.09	7.54	7.49
Fe	0.01	0.00	0.03	0.10	0.01	0.08	0.04	0.00	0.03	0.02
Mg	1.07	1.00	0.81	1.16	1.03	1.07	1.08	0.86	0.90	0.92
Sr	0.03	0.08	0.00	0.13	0.06	0.20	0.04	0.04	0.00	0.00
Ca	2.30	2.41	2.99	2.19	2.29	2.15	2.02	2.26	2.07	2.14
Na	0.11	0.10	0.14	0.24	0.16	0.21	0.15	0.25	0.31	0.53
K	0.38	0.53	0.46	0.56	0.62	0.74	0.38	0.39	0.71	0.68
Si/(Al+Fe)	3.82	3.65	3.30	3.42	3.43	3.38	4.03	4.08	3.78	3.80
E(%)‡	2.80	1.88	2.48	6.30	8.19	4.46	5.16	0.31	8.90	2.15

† Total iron.
‡ E(%): balance error.

tardi and Galli (1985), and are summarized in Table 2 and Figure 4. The compositional ranges of the 3 heulandite types are distinguishable from each other on the basis of Si/(Al+Fe) and (Na+K)/(Na+K+Ca+Mg) ratios (Figure 4).

Heulandite I has the lowest concentration of alkalies, and its Si/(Al+Fe) ratio ranges from 3.5 to 3.8. Heulandite II is less silicic, ranging in Si/(Al+Fe) from 3.2 to 3.6 and rather richer in (Na+K)/(Na+K+Ca+Mg). Both types of the heulandite generally show great variability in the Si/(Al+Fe) ratio from sample to sample and predominance of Ca as exchangeable cation, which are typical chemical characteristics of heulandite. In the heulandite I and II, however, no chemical variability was detected within the scale of a crystal.

Heulandite III is quite different in composition compared with the other types of heulandite. The heulandite III shows striking chemical zoning within a crystal, ranging from Si/(Al+Fe) ratio of 3.6 on the rim to 4.1

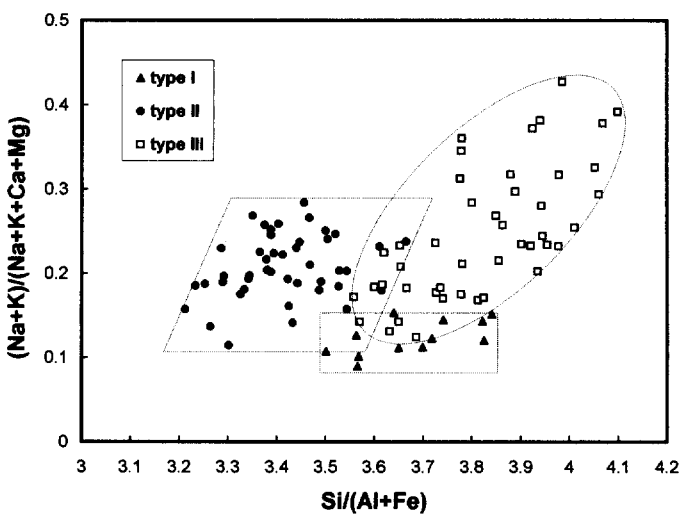

Figure 4. A correlation of Si(Al+Fe) vs. alkali abundance in the heulandite cements.

https://doi.org/10.1346/CCMN.1998.0460211 Published online by Cambridge University Press

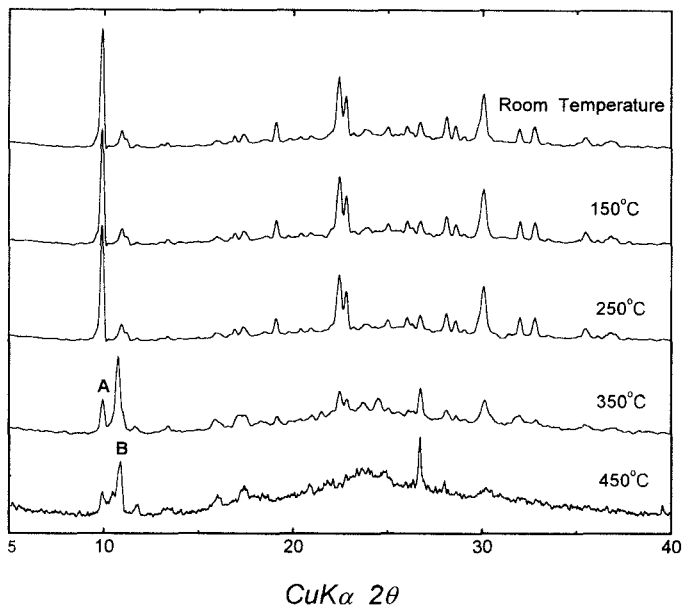

Figure 5. Comparison of XRD patterns of heulandite–clinoptilolite (heulandite III) at different temperatures: A) (020) reflection of natural phase of heulandite (heulandite A) and/or clinoptilolite, B) (020) reflection of high-temperature phase of heulandite (heulandite B).

in the center (Figure 4). Most analyses for the heulandite correspond to the compositional range of silicic heulandite, but some crystal center analyses are more silicic, ranging up to more than 4.0 in the Si/(Al+Fe) ratio, compatible with the clinoptilolite composition. The silicic part within a coarsely crystalline sample of the heulandite is comparable with the lower birefringent portions of the crystals. In addition, with increasing Si/(Al+Fe) ratio, considerable increase in (Na+K)/(Na+K+Ca+Mg), mainly in K abundance, occurs in the heulandite III (Figure 4).

XRD analysis on the heat-treated heulandite III at 350 °C during 12 h results in a major shift of (020) reflection from phase A (8.94 Å) to phase B (8.26 Å). But this high-temperature phase transition was not completed at 450 °C (Figure 5). A weak reflection at 8.94 Å, that is, (020) of a clinoptilolite phase, was sustained up to 600 °C. This reflects that the heulandite III forms a composite phase of heulandite and clinoptilolite, and the silicic lower-birefringent part of the heulandite III corresponds not to a heulandite but to a clinoptilolite phase. This type of heulandite is similar to the clinoptilolite crystals, showing uniform core and progressively zoned rim, found in the zeolitic tuff of the Barstow Formation (Sheppard and Gude 1969). But the heulandite–clinoptilolite is quite different in the modes of chemical zoning and occurrence of the zoned clinoptilolite from the Barstow Formation.

DIAGENETIC FEATURES AND PARAGENETIC SEQUENCE

The Chunbuk Formation has undergone shallow burial corresponding to a maximum burial temperature ranging between 40–60 °C, based on authigenic mineral facies and fission track thermochronology (Noh 1994; Shin and Nishimura 1994). Shallow burial and the presence of volcanic detritus in permeable sediments has resulted in crystallization of 3 types of heulandite cements in the fan-delta deposits. Paragenetic relationships among these heulandite phases cannot be deciphered directly, because they do not occur together in a specimen. However, some textural evidence and authigenic mineral associations make it possible to determine their paragenetic sequence (Figure 6).

The earliest generation of heulandite I can be inferred from the close association with the early-formed smectite together with unaltered glassy clayey matrix, and from its presence as remnants replaced by crystalline calcite cement (Figure 2B). In addition, the crystallization mode of heulandite I, that is, *in situ* alteration of the glassy matrix, suggests an early formation of the heulandite I. Compared to the heulandite I, heulandite II appears to have formed after the dissolution of carbonate cements during the later stage of burial diagenesis. This can be inferred from the fact that the heulandite II occurs as cavity-fillings associated with secondary porosity in the pore space of carbonate-free samples. The presence of clean boundaries between rimming heulandite II and detrital grains, without any early-formed diagenetic phases such as smectite, may also reflect the total dissolution of carbonate cements, either micritic or crystalline calcite, including small amounts of dolomite, prior to crystallization of heulandite II. Heulandite II may have

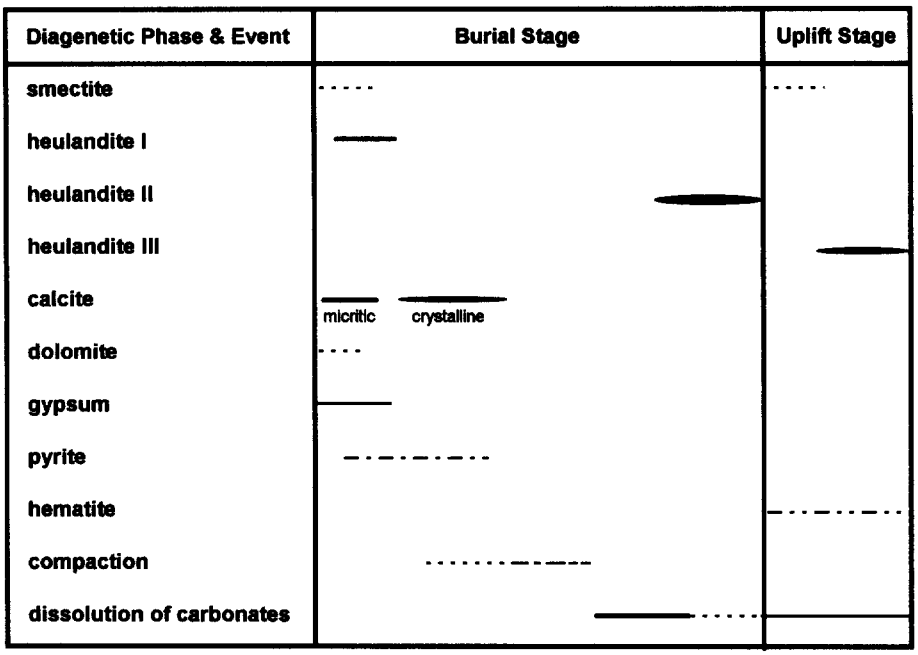

Figure 6. Paragenetic sequences of heulandite and other authigenic phases.

formed after slight compaction caused by the shallow burial, because the heulandite fills the interstitial cracks of dilated mica flakes.

Evidences that heulandite III formed after heulandite II is that late-formed smectite and hematite coatings postdate heulandite II but predate heulandite III (Figure 3). Smectite or the mixture of smectite and hematite, which frequently coats over the heulandite II, occurs between heulandite III and detrital grains, and less commonly, occurs as remnants within the heulandite III. The highly expandable smectite is frequently associated with reddish pigment-like hematite, which is presumably supergene in origin, forming typical coatings along the outline of detrital grains. Thus, the late-stage smectite coatings that formed prior to the precipitation of heulandite III appear to have formed during the uplift stage of the Chunbuk Formation. In addition, the unusual mode of occurrence of heulandite III, such as large single crystals, together with characteristic chemical zoning, may reflect that the heulandite III was formed during or after the uplift at somewhat diluted fluid conditions, presumably caused by the migration of meteoric water. This can be inferred from the general relation between nucleation and solution composition that as supersaturation decreases, both the rate of nucleation and the number of nuclei produced decrease, and the resulting precipitate tends to be coarser-grained (Walton 1967; Boistelle 1982; Morse and Casey 1988).

STRONTIUM ISOTOPE COMPOSITION AND FLUID SOURCES FOR HEULANDITE CEMENTATION

Calcium carbonates, plagioclase and volcanic material are generally important Sr sources in sandstone cements and commonly control the concentration and isotopic composition of Sr in pore fluids during diagenesis (Stanley and Faure 1979). Among these Sr sources, detrital calcium carbonates are obviously insignificant for the understanding of heulandite cementation in the area because of their absence in the fan-delta formation. In addition, the plagioclase is not important as a major source of Sr in the heulandite cements, because the input of plagioclase detritus in the sediments is minimal and, if present, very sodic ($Ab_{98\text{-}96}An_{2\text{-}4}$), and the plagioclase alteration such as albitization and dissolution is lacking due to the shallow burial and extensive early cementation of authigenic carbonates. In the heulandite cements, considering the lithology, sedimentary environment and the paragenetic sequence of diagenetic phases, volcanic detritus and early-formed authigenic carbonates may play major roles to control the concentration and isotope compositions of Sr in the heulandite cementation. The fluid composition at the time of heulandite cementation has resulted from the successive reactions of seawater with the unstable detrital volcanics and early-formed carbonates such as carbonaceous fossil tests and micritic calcite cement including calcite con-

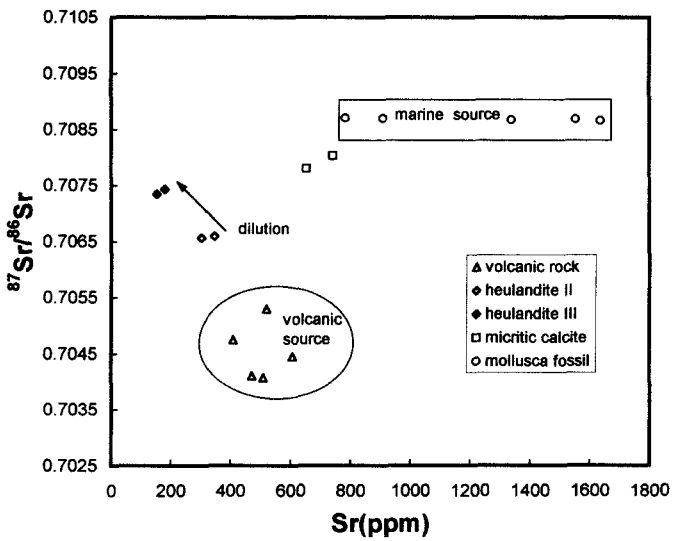

Figure 7. A diagram showing $^{87}Sr^{86}Sr$ ratio vs. Sr concentrations for heulandites, volcanic rocks and micritic carbonate cements and their correlation with the reported middle Miocene mollusca data (Woo and Park 1993).

cretions. These volcanic detritus and early-formed carbonates are considered as major Sr sources in the heulandite cements.

Among 3 types of heulandite cements, the Sr isotopic composition of heulandite I is presumably influenced largely by the Sr source of volcanic substance, because the Sr concentration of seawater entrapped as initial pore water at the time of deposition must have been too low to affect the Sr isotopic composition of heulandite I. Unfortunately, however, purified samples of the heulandite I could not be obtained for Sr isotope analysis. The Sr of marine source fixed into the earliest authigenic phases, that is, micritic carbonate phases and carbonaceous fossil tests, may significantly influence the formation of later-formed heulandite II and III. The concentrations and $^{87}Sr^{86}Sr$ ratios for the heulandite II and III, volcanic rocks and early-formed carbonates have been analyzed to evaluate the sources of fluid during heulandite cementation. These analyses are shown in Figure 7, together with values reported for unaltered mollusca by Woo and Park (1993).

The analyzed Sr isotope ratios (0.706565–0.707432) of 4 samples of heulandite II and III range nearly in the middle between values of volcanic rocks (0.704072–0.705298) and fossil mollusc (0.708670–0.708698). The Sr isotope data of micritic calcite cement (0.707801–0.708032) are slightly lower than those of the unaltered mollusc. As shown in Figure 7, each sample of both heulandites has similar values in Sr isotopic composition. Heulandite II is slightly lower ($^{87}Sr^{86}Sr$ ratio: 0.706565–0.706598) in terms of the Sr isotope composition and higher (347–304 ppm) in Sr concentration compared with heulandite III ($^{87}Sr^{86}Sr$ ratio: 0.707347–0.707432, Sr concentration: 152–179 ppm). These relations suggest that the chemistry of pore fluid during formation of heulandite cements was influenced by both marine and volcanic sources. The marine source of Sr was fixed together with Ca as micritic carbonate cements, and then, as the result from the dissolution of carbonate cements and carbonaceous fossils, it in part contributed to the formation of heulandite II and III at the later stage of diagenesis. The dissolution of these carbonates in sandstones can be caused by migration of meteoric water during burial and uplift (Mathiesen 1984; Surdam et al. 1984; Remy 1994). The entrapped seawater in sediments may be a primary source of Sr of marine origin, but its concentration of Sr is too low to significantly affect the fluid composition of pore fluid to control the heulandite cementation.

Considering the basin geology, lithology and the Sr analyses, 2 potential sources for Sr of volcanic origin can be postulated to understand the Sr sources of the pore fluid relating to the heulandite cementation. These are caused by a subsequent alteration of volcanic detritus during burial and an input by the migration of meteoric water from tuffaceous volcanic rocks overlain by the fan-delta formation. Coarse-grained texture of the sediments and later dissolution of the early-formed carbonates may provide a favorable condition for an active migration of meteoric water into pore fluid, presumably at the stage of the formation of heulandite II and III. The higher $^{87}Sr^{86}Sr$ ratio and lower Sr concentration of heulandite III, compared to those of heulandite II, may indicate that meteoric water migration and subsequent carbonate dissolution have occurred progressively during the formation of these pore-filling zeolite cements. In addition to the alterations of volcanic detritus in sediments, the meteoric groundwater circulated within tuffaceous dacitic

volcanics seems to provide additional chemical components such as Si and Al necessary for heulandite formation into the pore fluid within sediments.

A correlation of Sr isotope data and Sr concentrations of the heulandite II and III with those of volcanic and marine sources may reflect that the heulandite III was much more influenced by meteoric water and formed at somewhat diluted condition in fluid composition. In addition, the late-formed smectite coating and hematite precipitation prior to the heulandite III indicate that the heulandite III was probably formed during or after uplifting of the fan-delta formation from oxygen-rich meteoric water. The dilution of pore fluid incursion of meteoric water may suppress nucleation, resulting in unusual coarse crystals and chemical zoning of the heulandite III. The successive dissolution during uplift of early-formed marine carbonate cements inevitably provided a marine Sr component in the diluted pore water. As a result, heulandite III seems to have a slightly higher $^{87}Sr/^{86}Sr$ ratio than heulandite II.

SUMMARY AND CONCLUSIONS

Heulandite was diagenetically formed as *in situ* alterations (heulandite I) and pore-fillings (heulandite II and III) in the conglomerate and sandstone of the fan-delta system. The first type of heulandite, heulandite I, occurs as replacements of volcanic and clayey matrix. Heulandite II, the main type of the heulandite cements, was formed as fillings in intergranular cavities after the compaction and carbonate dissolution during burial. The heulandite III, heulandite–clinoptilolite, which occurs as coarse-crystalline single-crystal cement, is a composite phase of heulandite and clinoptilolite, showing a chemical zoning ranging from 3.6–4.1 in Si/(Al+Fe) ratio.

Heulandite formation in the fan-delta sediments was initiated by the interaction of volcanic detritus and entrapped seawater during burial. High porosity of coarse-grained sediments of the fan-delta system may have facilitated the alteration of volcanic matrix to heulandite I during the early stage of diagenesis, despite the low-temperature (40–60 °C) diagenetic regime and the epiclastic input of silicic volcanic detritus in sediments. Due to the lower abundance of volcanic detritus and the lack of volcanic glass such as glass shards, compared to typical volcaniclastic sandstones, this alteration reaction continued sluggishly and incompletely throughout the diagenetic regime. Early cementation of micritic carbonates that occurred prior to burial also played a role in retarding the alteration by preventing the fluid access to volcanic detritus in the beginning stage of burial diagenesis.

The leached pore fluid from the alteration of volcanic detritus to heulandite I primarily provided necessary ions for the later-formed pore-filling heulandite II and III. The high porosity of the fan-delta system made it possible to provide additional components such as Si and Al necessary for the later formation of heulandite cements, largely by the migration of meteoric water percolating from tuffaceous volcanic basement through residual volcanic detritus in sediments. Based on the paragenetic sequences of authigenic phases and their Sr isotope data, the major cation in the pore-filling heulandite cements, Ca, was largely derived from the dissolution of incipient carbonate cements.

The frequent recharge of meteoric water into the fan-delta formation and subsequent dissolution of carbonate cements controlled the later formation of coarsely crystalline heulandite cements. During burial and uplift of the fan-delta system, mixing and dilution of pore fluid with pervasive meteoric water resulted in the formation of characteristic heulandite II and III of the fan-delta formation. The unusual coarse and characteristic single-crystal cementation of heulandite III appears to be related to the supergenic formation of heulandite during or after uplifting at diluted pore water conditions with oxygen-rich meteoric water. A chemical zoning of the heulandite III may indicate that the heulandite–clinoptilolite phase formed at a disequilibrium condition and the ambient fluid composition at that time of crystallization of the heulandite III had changed with decreasing in Si/Al ratio.

ACKNOWLEDGMENTS

This work has been financially supported by the Yonam Foundation of Korea. Financial support was also provided in part by KOSEF (KOSEF 94-0703-04-01-3). I am greatly indebted to J. R. Boles, R. L. Hay, and T. L. Dunn for their critical readings of the manuscript and helpful comments. I am grateful to K. H. Park and I. S. Lee of the Korea Basic Science Institute for their cooperation in isotope analysis. I also thank D. Pierce for his assistance with electron microprobe works.

REFERENCES

Alietti A. 1972. Polymorphism and crystal chemistry of heulandites and clinoptilolites. Am Mineral 57:1448–1462.

Alietti A, Gottardi G, Poppi L. 1974. The heat behavior of the cation exchanged zeolites with heulandite structure. Tscher Mineral Petrogr Mitteil 19:291–298.

Boistelle R. 1982. Mineral crystallization from solution. Estudios Geologie 38:135–153.

Boles JR. 1972. Composition, optical properties, cell dimensions and thermal stability of some heulandite group minerals. Am Mineral 57:1463–1493.

Chough SK, Barg E. 1987. Tectonic history of Ulleung Basin margin, East Sea (Sea of Japan). Geology 15:45–48.

Chough SK, Hwang IG, Choe MY. 1990. The Miocene Doumsan fan-delta, southeast Korea: A composite fan-delta system in back-arc margin. J Sedi Petrol 60:445–455.

Gottardi G, Galli E. 1985. Natural zeolites. Berlin: Springer-Verlag. 380 p.

Hay RL. 1966. Zeolites and zeolitic reactions in sedimentary rocks. Geol Soc Am Spec Paper 85. 130 p.

Hwang IG. 1993. Fan-delta systems in the Pohang Basin (Miocene), SE Korea [Ph.D. thesis]. Seoul, Korea: Seoul National Univ. 923 p.

Hwang IG, Chough SK. 1990. The Miocene Chunbuk Formation, southeastern Korea: Marine Gilbert-type fan-delta system. Spec Publ Int Assoc Sedimentol 10:235–254.

Iijima A, Utada M. 1971. A critical review on the occurrence of zeolites in sedimentary rocks in Japan. Jpn J Geol Geogr 42:61–83.

Lander RH, Hay RL. 1993. Hydrogeologic control on zeolitic diagenesis of the White River sequence. Geol Soc Am Bull 105:361–376.

Mathiesen ME. 1984. Diagenesis of Plio-Pleistocene nonmarine sandstones, Cagayan basin, Philippines: Early development of secondary porosity in volcaniclastic sandstones. In: McDonald DA, Surdam RC, editors. Clastic diagenesis. Am Assoc Petrol Geol Memoir 37. p 177–193.

Morse JW, Casey WH. 1988. Ostwald process and mineral paragenesis in sediments. Am J Sci 288:537–560.

Mumpton FA. 1960. Clinoptilolite redefined. Am Mineral 45: 351–369.

Noh JH. 1994. Stratigraphy, lithology and diagenetic mineral facies of the Tertiary Yeonil Group. Korea J Petrol Geol 2: 91–99 (in Korean).

Noh JH, Boles JR. 1989. Diagenetic alteration of perlite in the Guryongpo area, Republic of Korea. Clays Clay Miner 37:47–58.

Noh JH, Boles JR. 1993. Origin of zeolite cement from the Miocene sandstones in the North Tejon oil field, California. J Sedi Petrol 63:248–260.

Remy RR. 1994. Porosity reduction and major controls on diagenesis of Cretaceous-Paleocene volcaniclastic and arkosic sandstone, Middle Park Basin, Colorado. J Sedi Res A64:797–806.

Sheppard RA, Gude AJ. 1969. Diagenesis of tuffs in the Barstow Formation, Mud Hills, San Bernardino County, California. US Geol Surv Prof Paper 634. 34 p.

Shin S, Nishimura S. 1994. Thermotectonic and sedimentation history of the Pohang Basin, Korea assesed by fission track thermochronology of a deep borehole granite. Korea J Petrol Geol 2:9–17.

Stanley KO, Faure G. 1979. Isotopic composition and sources of strontium in sandstone cements: The high plains sequence of Wyoming and Nebraska. J Sedi Petrol 49:45–54.

Surdam RC, Boese SW, Crossey LJ. 1984. The Chemistry of secondary porosity. In: McDonald DA, Surdam RC, editors. Clastic diagenesis. Am Assoc Petrol Geol Memoir 37. p 127–149.

Surdam RC, Boles JR. 1979. Diagenesis of volcanic sandstones. In: Scholle PA, Schluger PR, editors. Aspects of diagenesis. SEPM Spec Publ 26. p 227–242.

Walton AG. 1967. The formation and properties of precipitates. New York: Intersci. Publ. 232 p.

Woo KS, Park KH. 1993. Sr isotope ages of well preserved molluscs from the Chunbuk Formation (Pohang basin) and the Shinhyon Formation (Yangnam basin). J Geol Soc Korea 29:187–214.

(Received 23 May 1997; accepted 26 August 1997; Ms. 97-044)